Marine Micropaleontology 136 (2017) 37–50

Contents lists available at ScienceDirect

Marine Micropaleontology

journal homepage: www.elsevier.com/locate/marmicro

Research paper

Calcification depths of planktonic foraminifera from the southwestern Atlantic derived from oxygen isotope analyses of sediment trap material

I.M. Venancio[a,b,*], A.L. Belem[c], T.P. Santos[b], D.O. Lessa[b], A.L.S. Albuquerque[b], S. Mulitza[a], M. Schulz[a], M. Kucera[a]

[a] MARUM—Center for Marine Environmental Sciences, University of Bremen, Bremen, Germany
[b] Departamento de Geoquímica, Universidade Federal Fluminense, Outeiro de São João Batista, s/n, Niterói, Rio de Janeiro 24020-141, Brazil
[c] Departamento de Engenharia Agrícola e Meio Ambiente, Universidade Federal Fluminense, Niterói, Rio de Janeiro 24210-240, Brazil

ARTICLE INFO

Keywords:
Planktonic foraminifera
Seasonality
Sediment traps
Western boundary current
South Atlantic

ABSTRACT

We present a multi-year record of shell fluxes and $\delta^{18}O$ of six planktonic foraminifera species (*Globigerinoides ruber* pink, *Globigerinoides ruber* white, *Trilobatus sacculifer*, *Orbulina universa*, *Neogloboquadrina dutertrei*, *Globorotalia menardii*) from sediment traps located in the southwestern Atlantic. Among the six species, only the fluxes of *G. ruber* white and *N. dutertrei* exhibit a significant seasonal component, with *G. ruber* white showing a single flux peak in austral summer, and *N. dutertrei* exhibiting two flux peaks in spring and autumn. To estimate calcification depths of the studied species, we then compare their measured $\delta^{18}O$ to vertical $\delta^{18}O$ profiles predicted for each collection time from in-situ temperature profiles and climatological salinity profiles. For the majority of the cases, the measured $\delta^{18}O$ could be accounted for by in-situ calcification, assuming species-specific temperature-$\delta^{18}O$ calibrations. The resulting estimates of the calcification depth imply that each species exhibits a characteristic typical mean calcification depth. The estimated calcification depths for *N. dutertrei* (mode 60–70 m) and *G. menardii* (mode 70–80 m) appear to track the depth of the thermocline in the region, whereas the calcification depths of the remaining four species correspond to conditions in the mixed layer. Among the apparent mixed-layer calcifiers, *G. ruber* pink and white appeared to calcify consistently shallower (mode 30–40 m) while *T. sacculifer* calcified deeper (mode 50–60 m). Because of the low flux seasonality, the observed oxygen isotope offsets among the species are similar to the flux-weighted mean annual $\delta^{18}O$ offsets, indicating that isotopic offsets among the species in sediment samples are mainly due to different calcification depths. Since the habitat offsets among the species are consistent across seasons, $\delta^{18}O$ in sedimentary shells can be used to track conditions in different parts of the water column and the difference in the oxygen-isotope composition between surface species (best represented by *G. ruber* pink) and thermocline species (best represented by *N. dutertrei*) can be used as a proxy for stratification in the southwestern Atlantic.

1. Introduction

Our ability to reconstruct past oceanographic conditions depends on the understanding of how ocean properties are recorded by proxies. One of the most widely used proxies in paleoceanography is the oxygen-isotopic composition ($\delta^{18}O$) of planktonic foraminifera in marine sediments, which is used to estimate changes in $\delta^{18}O$ of seawater and temperature (Duplessy et al., 1991; Bemis et al., 2002). Since planktonic foraminifera species inhabit different depth habitats, which may vary temporally and spatially, and change during the life of each individual (Rebotim et al., 2017), assessments of their vertical habitats and especially the calcification depth is crucial for paleoceanography. Without knowledge of calcification depths, environmental conditions reconstructed from the chemical composition of foraminiferal shells cannot be assigned to the part of the water column, where the signals were generated. Since living depths (Rebotim et al., 2017) and by inference also calcification depths of planktonic foraminifera vary in response to environmental conditions, regional assessments, especially in areas that lacks this type of information, are needed to provide the basis for interpretations of the proxy signals in the fossil record. If species could be identified that consistently calcify in different parts of the water column, multi-species proxy data could be used to evaluate past changes in the stratification of the upper water column (Williams and Healy-Williams, 1980; Mulitza et al., 1997).

A powerful means of constraining the origin of isotopic signatures in planktonic foraminifera is by analysis of shells from sediment-trap time-

* Corresponding author at: MARUM—Center for Marine Environmental Sciences, University of Bremen, Bremen, Germany.
E-mail address: ivenancio@marum.de (I.M. Venancio).

http://dx.doi.org/10.1016/j.marmicro.2017.08.006
Received 12 January 2017; Received in revised form 29 August 2017; Accepted 30 August 2017
Available online 04 September 2017
0377-8398/

series, which are an effective method to constrain the effect of flux seasonality (Jonkers et al., 2010; Žarić et al., 2005). Studies using sediment traps have shown changes in planktonic foraminifera assemblages and shell fluxes (Thunell and Sautter, 1992; King and Howard, 2005; Jonkers et al., 2010) as well as changing calcification depths (Wejnert et al., 2013) throughout the seasonal cycle. These observations imply that planktonic foraminifera may adapt their habitat in order to stay within a preferred temperature range (Jonkers and Kucera, 2015). Thus, their calcification habitat can only be constrained by sampling at sufficient seasonal resolution with simultaneous recording of vertical temperature gradients above the sediment trap. In this respect, a deeply moored sediment trap collects foraminifera from a potentially large catchment area, which may include spatially variable vertical water column structure. Therefore, estimates of calcification depth from a shallow moored trap are likely to better constrain calcification habitat.

In this study, we use a sediment trap record from the southeastern continental shelf off Brazil to derive shell fluxes and $\delta^{18}O$ of the planktonic foraminifera species *Globigerinoides ruber* white, *Globigerinoides ruber* pink, *Trilobatus sacculifer*, *Orbulina universa*, *Globorotalia menardii*, and *Neogloboquadrina dutertrei*. The mooring was operated over four years with traps moored between 50 and 100 m depth, minimizing the potential catchment area. Instead of relying on data from unevenly spaced and scattered CTD profiles (Jonkers et al., 2010) or on information from climatological oceanographic data (Gibson et al., 2016), simultaneous in situ recording of the vertical temperature profile was available throughout the sampling period, allowing direct comparison of shell chemistry with local hydrography. By sampling over all four seasons (replicating three seasons), we can effectively investigate the seasonal variation of calcification depths. Combining calcification depths with flux data allows us to evaluate the implications of the sediment trap observations for paleoceanographic records.

2. Materials and methods

2.1. Sediment trap sampling

The mooring line that was available for the study was deployed within the Brazilian Project *Ressurgência*. The mooring is located over the Brazilian southeastern continental shelf at 23°36′ S, 41°34′ W (Fig. 1) at a water depth of 145 m. Sediment traps were positioned at depths of 50 and 100 m (first to fourth deployment) and 75 m (single trap, sixth and seventh deployments). The used sediment traps PARFLUX (model Mark 8–13) have an aperture of 0.25 m^2 and 12 or 13 sequential bottles with 500 ml capacity. Each sample bottle was filled with pre-filtered MilliQ water with buffered (pH = 8) formaldehyde (4%) after adjusting the salinity with marine salt (RedSea©) to 70 PSU to prevent mixing and bacterial decomposition of collected particles (Goswami, 2004). In addition to the traps, the mooring line contained temperature loggers (ONSET tidbits V2) between 30 m and 120 m, spaced at 5 m intervals and two current meters (400 kHz Nortek Aquadopp Profilers) configured to up and down looking acoustic current profiling. The physical parameters (temperature and velocities) were measured at 30-minute intervals. In general, our mean current velocities are higher than 12 cm/s with a strong along-shelf component towards the south, but with the current velocity and direction remaining relatively stable between the deployments. Regarding the recorded temperature (Supporting information Fig. S3), the 100-m trap is more influenced by water masses with temperatures below 18 °C, while the shallow traps (50 and 75-m) are in contact with waters that have temperature higher than 18 °C, but subsurface intrusions can bring cold waters to these shallower traps as well. A detailed description of the temperature, current-meter data (trap efficiency) and bulk composition was previously published (Albuquerque et al., 2014; Belem et al., 2013; Venancio et al., 2016a).

The samples and data used in this study were retrieved during six deployments between November 2010 and March 2014 (Table 1). Sampling resolution varied among the deployments. The first experiment (F1) was from November 11th to December 19th 2010 (3-day sampling rate). The second experiment (F2) was from March 15th to June 14th 2011 (7-day sampling rate). The third experiment (F3), from July 20th to September 26th 2011 (5-day sampling rate) and the forth experiment (F4) covered the time frame between December 2nd 2011 and March 2nd 2012 (7-day sampling rate). Samples for the fifth experiment were not used due to technical problems in the equipment. The sixth experiment (F6) was from June 9th to September 8th 2013 (7-day sampling rate) and the seventh experiment (F7) covered the time frame between September 15th of 2013 and March 16th of 2014. Gaps in the time series were caused by operational constraints in recovering the experiments.

2.2. Sample treatment

The sediment trap samples were wet-sieved through 1 mm and 500 μm meshes before being split into four aliquots. A Folsom's plankton sample divider was used for splitting the samples. The volume of the resulting aliquots was determined to adjust the split factor used to calculate the concentration of foraminifera in the total sample. For deployments 1–4, a split factor close to 4 was used to calculate the foraminiferal fluxes, while for deployment 6–7 split factors were more variable ranging from 5.6 to 7.7. After wet-sieving, the > 125 μm fraction was used for species identification and counting. This size fraction was chosen because it covers the size range of most recent species and also contains all foraminifera > 150 μm, which are usually used for paleoceanographic studies (Al-Sabouni et al., 2007; Žarić et al., 2005). The samples were analyzed wet allowing the counting of fragile shells which could disintegrate during drying. Wet-picking was performed using a transparent gridded tray for zooplankton analysis. The species *G. ruber* (pink and white), *T. sacculifer* (without sac-chamber), *O. universa*, *G. menardii* and *N. dutertrei* were the most abundant, representing > 70–80% of the assemblage in most samples, and were therefore analyzed further in this study. The remaining part of the assemblage is composed by *Globigerinella siphonifera*, *Globigerinoides conglobatus*, *Globigerina bulloides*, *Globigerinita glutinata*, *Globoturborotalita rubescens* and *Globigerinella calida*, with minor contributions by *Turborotalita quinqueloba*, *Globoturborotalita tenella* and *Globorotalia truncatulinoides*. The taxonomy of *Trilobatus sacculifer* follows the proposal of Spezzaferri et al. (2015). Whereas the two color varieties of *G. ruber* (white and pink) were separated, no distinction was made between *G. ruber* and *G. elongatus* (Aurahs et al., 2011). Planktonic foraminifera fluxes from the first to the fourth deployment were previously published by Venancio et al. (2016a). Flux data for the remaining deployments will be made available at Pangaea (www.pangaea.de).

For the oxygen isotopic analysis, 5–10 specimens of each of the chosen species were selected. Because in many of the sampling intervals, the flux of the studied species was low, the analyses could not be carried out specifically for a narrow size fraction. Instead, the size of the measured specimens was recorded by measuring the length of the major axis of the shells and varied for *G. ruber* pink (280–720 μm), *G. ruber* white (280–720 μm), *T. sacculifer* (400–800 μm), *N. dutertrei* (320–760 μm), *O. universa* (520–960 μm) and *G. menardii* (520–960 μm). Stable oxygen isotopes were analyzed with a Finnigan MAT 252 mass spectrometer coupled to an automated carbonate preparation device at MARUM, University of Bremen. The isotopic results were calibrated relative to the Vienna Pee Dee Belemnite (VPDB) by using the NBS 19 standard. The long-term analytical standard deviation was < 0.07‰. All data, including sizes of the measured specimens will be made available at Pangaea (www.pangaea.de).

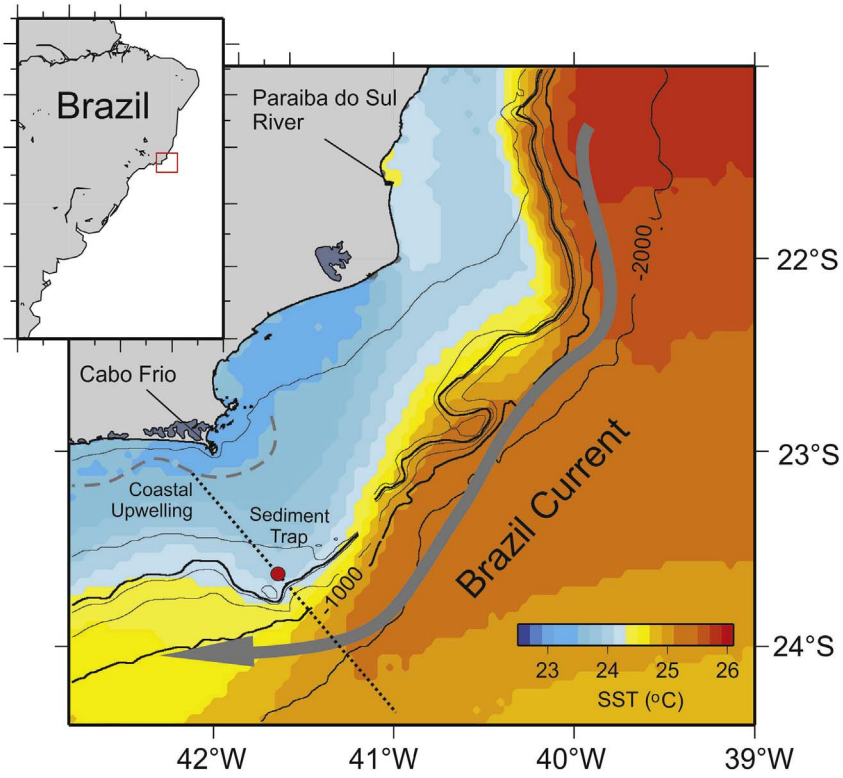

Fig. 1. Study area and oceanographic features. The mooring site is marked with a red circle. The color scale represents the distribution of 10-year mean sea surface temperature. Data was extracted from the AVHRR dataset (AVHRR Pathfinder v.5). (For interpretation of the references to color in this figure legend, the reader is referred to the web version of this article.)

Table 1
Mooring configurations for each of the deployments.

Deployments	Trap depths (m)	N° of cups analyzed	Time interval		Sample integration (days)
			Start	End	
F1	50; 100	12	11 Nov 2010	19 Dec 2010	3
F2	50; 100	12	15 Mar 2011	14 Jun 2011	7
F3	50; 100	12	20 Jul 2011	26 Sep 2011	5
F4	50; 100	12	02 Dec 2011	02 Mar 2012	7
F6	75	13	09 Jun 2013	08 Sep 2013	7
F7	75	13	15 Sep 2013	16 Mar 2014	14

2.3. Evaluation of seasonal cycles

Shell fluxes of each species, sea surface temperatures (SST) from the Advanced Very High Resolution Radiometer (AVHRR) dataset, temperatures recorded by the mooring and the estimations of calcification depths (see Section 2.4) were tested for the presence of seasonal cycles using a periodic regression analysis. For the analysis of the shell flux data we used the deployments 2 (100 m trap), 6 and 7 that cover all seasons and also have sampling time integrations ranging from 7 to 14 days, which avoids the interference of short-term flux variations. The models generated using these three deployments (2, 6 and 7) were then applied to the entire dataset. The mooring temperatures were binned in 10-meter sections starting at 30 m, first level of measurements available, and ending at 100 m, which is the depth of the deepest sediment trap. Both AVHRR-SST and mooring temperatures were analyzed as daily averages covering the entire time series. For the calcification depths the entire dataset was analyzed.

In the periodic regression analysis the independent variable is an angular representation of time and this approach was demonstrated to be robust for detection of lunar periodicity (deBruyn and Meeuwig, 2001) and seasonality (Bell et al., 2001; Jonkers and Kucera, 2015). Furthermore, the analysis gives information about the timing of the maximum in the dataset and provides an equation which can be used to estimate values for a given period. The methods and advantages in detecting lunar and seasonal cycles are summarized by deBruyn and Meeuwig (2001) and Jonkers and Kucera (2015), respectively. Regarding the shell fluxes, we followed Jonkers and Kucera (2015) and performed a log transformation of the flux data prior to the analysis. To facilitate the log transformation, zero flux values were replaced by half of the second lowest flux value for each deployment, also following Jonkers and Kucera (2015). The observation time was converted to days of the year (DOY) and transformed in radian units (DOY/365 × 2π). In order to test the cycles the following models were applied to observations:

$$F_{(t)} = A + B_{\sin(t)} + C_{\cos(t)}$$

$$F_{(t)} = A + D_{\sin(2t)} + E_{\cos(2t)}$$

where $F_{(t)}$ is the shell flux or temperature at a given time and A–E are the parameters that will be estimated in the analysis. The statistical significance of the terms of the periodic regression analysis was evaluated using ANOVA for multiple regression.

2.4. Calcification depths and flux-weighted $\delta^{18}O$

In order to estimate the calcification depths for each species, we applied species-specific paleotemperature equations and inverted these to predict the $\delta^{18}O$ of the calcite ($\delta^{18}O_{predicted}$) from the in-situ temperature profiles, $\delta^{18}O$ of seawater ($\delta^{18}O_{sw}$) was calculated using monthly salinity values from the World Ocean Atlas 2013 (WOA13) and the $\delta^{18}O_{sw}$-salinity relationship derived from the dataset of Pierre et al. (1991). This $\delta^{18}O_{sw}$-salinity was previously used for salinity reconstructions in the Brazilian margin by Toledo et al. (2007). The $\delta^{18}O_{sw}$ values were converted from VSMOW to VPDB by subtracting 0.27‰ (Hut, 1987) from the values derived from Eqs. (1), (2) and (5). In the case of the Eqs. (3) and (4) we subtracted 0.20‰ (Bemis et al.,

1998). Since we used monthly salinity values for our $\delta^{18}O_{sw}$ estimations, sub-monthly and interannual variability was not considered. The assumption of this approach is that the collected planktonic foraminifera calcified during the sampling period in the studied area. The species-specific paleotemperature equations are as follows:

$$T\,(°C) = 14.2 - 4.44 \times (\delta c - \delta sw) \quad (1)$$

$$T\,(°C) = 14.91 - 4.35 \times (\delta c - \delta sw) \quad (2)$$

$$T\,(°C) = 15.4 - 4.81 \times (\delta c - \delta sw);\ (\text{Bouvier-Soumagnac and Duplessy, 1985}) \quad (3)$$

$$T\,(°C) = 14.6 - 5.03 \times (\delta c - \delta sw);\ (\text{Bouvier-Soumagnac and Duplessy, 1985}) \quad (4)$$

$$T\,(°C) = 16.5 - 4.8 \times (\delta c - \delta sw);\ (\text{Bemis et al., 1998}) \quad (5)$$

Eq. (1) was used for *G. ruber* (pink and white), Eq. (2) for *T. sacculifer*, Eq. (3) for *O. universa*, Eq. (4) for *G. menardii* and Eq. (5) for *N. dutertrei*. In all cases, except *N. dutertrei*, we used equations derived from plankton tow studies. For *N. dutertrei* we use the equation derived from a culture study using *O. universa* at low-light conditions (Bemis et al., 1998). The species-specific equation for *N. dutertrei* from Bouvier-Soumagnac and Duplessy (1985) is known to produce estimates that are too cold (Wejnert et al., 2013). It indeed generated unrealistic values for the region and was therefore not used. Alternative equations based on plankton tow calibrations exist for some of the species, but these differ only marginally (e.g., Wejnert et al., 2013).

Profiles of $\delta^{18}O_{predicted}$ with their respective measured $\delta^{18}O$ for *G. ruber* white are shown as examples of our calcification depth approach (Supporting information Fig. S4). We used the maximum and minimum temperatures from each depth interval to generate the $\delta^{18}O_{predicted}$ profiles for a given period (Supporting information Fig. S4). Since the studied foraminifera may have calcified different portions of their shell at different times and depths, the resulting isotopic composition is reflecting the average conditions in the total calcification habitat. It is difficult to constrain the effect of calcification across habitats precisely, which is why we opted for a conservative approach and estimated the possible range of calcification depths by determining the deepest and shallowest possible calcification depth given the temperature variation during the sampling interval, when the analyzed foraminifera lived.

Considering the analytical error of $\delta^{18}O$ measurements and the statistical uncertainties of the $\delta^{18}O_{sw}$-salinity and paleotemperature equations, we can estimate the magnitude of uncertainty for a calcification depth value due to these processes. For example, taking the $\delta^{18}O$ value of *G. ruber* white for a sample (6th bottle of 50-m in the 1st deployment) and representing the calcification temperature range by a mean profile throughout the sampling interval, we estimate an error on the calcification depth estimate due to analytical error and calibration uncertainty of 16.7 m. Using an approach based only on the temperature profile variation yields an uncertainty of 16.4 m. For deeper layers, the uncertainty due to variation within the sampling interval will be larger than the uncertainty due to calibration, because temperature variation is higher reflecting the changes in thermocline depth, whereas calibration uncertainty remains the same. Thus, by showing the range of possible calcification depths based on minimum and maximum temperatures during a given sampling period, we are making a conservative approach that is equivalent to error estimates. Calcification depths for the entire time series were further evaluated for seasonal component using periodic regression analysis (Section 2.3).

Next, to assess the effect of seasonal fluxes on the mean $\delta^{18}O$ signal exported to the sediments, we determined the flux-weighted annual $\delta^{18}O$ values for each of the chosen species. The fundamentals of this approach were discussed by Mulitza et al. (1998), using the model proposed by Mix (1987). The flux-weighted annual $\delta^{18}O$ values were calculated using the following equation:

$$Fw = \sum_{i=1}^{n} (flux_i \times \delta c_i) \Big/ \text{total flux}$$

where Fw is the flux-weighted $\delta^{18}O$ value, $flux_i$ and δc_i are the shell flux and the $\delta^{18}O$ of calcite in a specific sample, respectively.

3. Oceanographic setting

The mesoscale surface circulation of the western boundary of the South Atlantic is dominated by the warm and nutrient-poor Brazil Current (Peterson and Stramma, 1991). As discussed by Walsh (1988), continental shelves located in the tropics and linked to the western edge of oceanic systems are often related to less productive oceanic margins. However, mesoscale processes related to the dynamics of Brazil Current (BC) (encroachment, topographic acceleration, meandering and eddies) may induce the upwelling of cold and nutrient-rich South Atlantic Central Water (SACW) on the shelf, forming an upwelling system in the southeastern portion of the Brazilian shelf (Belem et al., 2013; Campos et al., 2000; Castelao and Barth, 2006; Silveira et al., 2008). This upwelling system (Cabo Frio Upwelling system-CFUS) is one of the most productive areas of the southeastern Brazilian shelf. Despite the control of the nutrient-poor western boundary BC, it interacts with the instabilities of the southward trajectory of the BC carrying oligotrophic Tropical Waters (Belem et al., 2013) and with the wind-driven coastal Ekman transport (Castelao and Barth, 2006), and allows a mid-shelf eddy-induced cold-water intrusion of South Atlantic Central Water (SACW) to the photic zone (Brandini, 1990; Campos et al., 2000; Calado et al., 2010). Following Albuquerque et al. (2014), the complex interactions of such system leads to a heterogeneous pattern of primary productivity (Franchito et al., 1998; Lopes et al., 2006), recycling and transport of particulate material on the shelf.

The continental shelf circulation off southeastern Brazil (Fig. 1), especially between 21°S and 25°S, has been widely studied due to this upwelling system (Ikeda et al., 1974; Rodrigues and Lorenzzetti, 2001; Castelao and Barth, 2006; Castelao, 2012; Castro, 2014; Cerda and Castro, 2014). The BC flows southward along the shelf break and slope of the Brazilian margin, as a component of the South Atlantic subtropical gyre, acquiring intensity and speed southward of the Abrolhos Bank (Silveira et al., 2000). This boundary current carries Tropical Water (TW) at the upper layers of the water column, as well as the South Atlantic Central Water (SACW) at an intermediate depth southwards (Fig. 1; Stramma and England, 1999). The BC exhibits an annual cycle in SST in our study area, where SST values range from 26 °C in March, to 22 °C during August and September. Regional hydrographic data also point to similar seasonal temperature variation at our study site (Cerda and Castro, 2014; Chiessi et al., 2014). As pointed out by Chiessi et al. (2014), variations in surface salinity are less pronounced than temperature during the annual cycle. In fact, the shallower trap (50 m) is more influenced by the TW and the deeper trap (100 m) by the SACW. The material collected by the deeper trap (100 m) is derived from both layers, while the shallower trap (50 m) material is mostly derived from the surface layer (TW), although SACW intrusions can be identified on the temperature dataset for both traps. TW and SACW, besides the Coastal Water (CW) and the Subtropical Shelf Water (STSW), are the main water masses at the upper part of the water column of the southeastern Brazilian margin (Castro, 2014; Venancio et al., 2014). Our recorded mean temperature profile (supporting information Fig. S3) also shows that a shoaling of the thermocline (18 °C isotherm) is more frequent during spring and autumn, with a strong deepening during the winter. As pointed out by Belem et al. (2013), the subsurface temperature variability in this area is influenced by several mechanisms, with the proximity of the BC to the shelf break being the most dominant factor modulating the temperatures at the top 80 m.

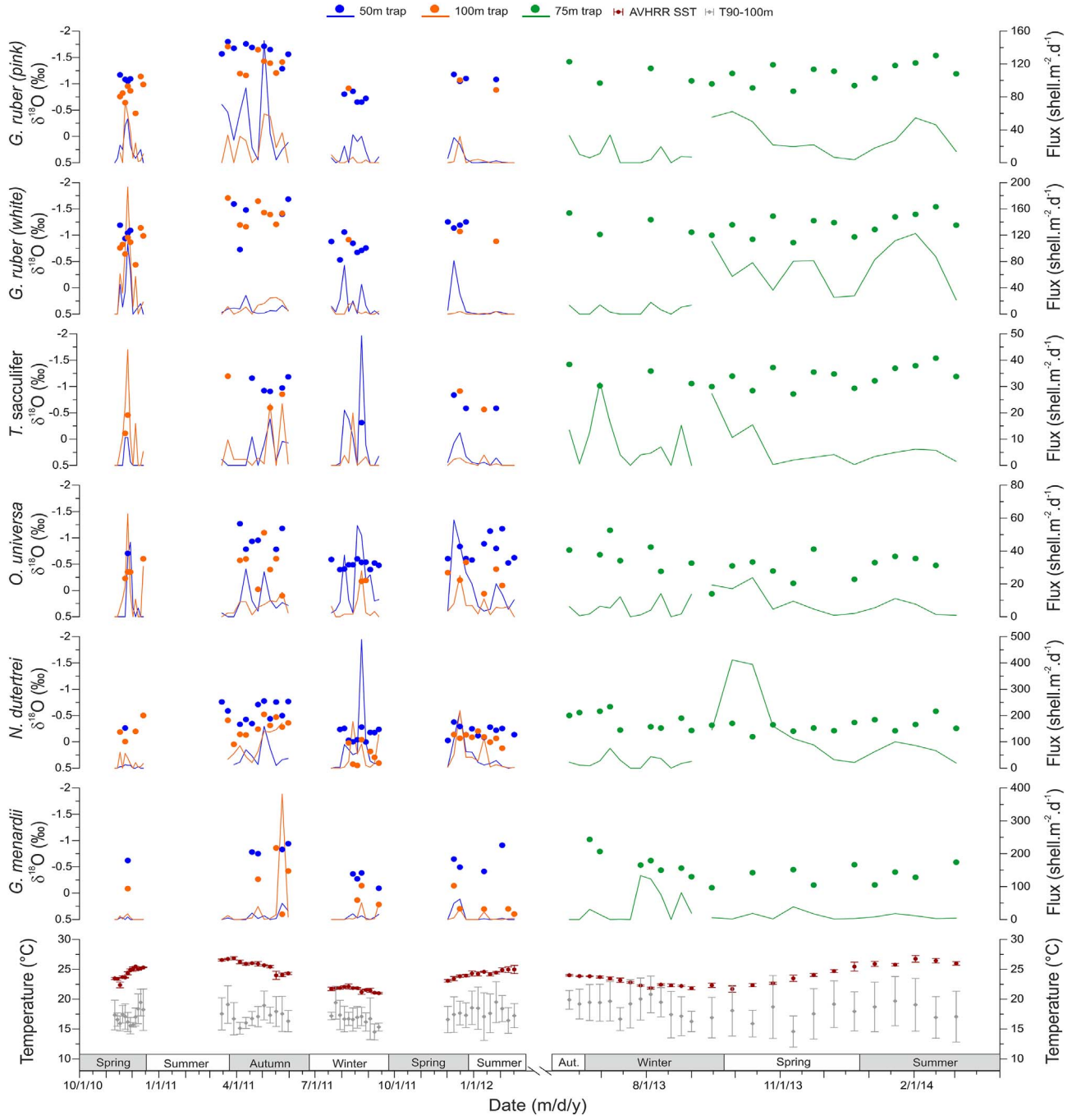

Fig. 2. Shell fluxes, oxygen isotope ratios of the planktonic foraminifera species and temperature records. The shell fluxes are plotted as lines in blue (50 m), orange (100 m) and green (75 m). Shell fluxes axes are variable between species. The oxygen isotopes are plotted as circles with the same color representation for each trap depth as the fluxes. The lowest panel displays the AVHRR-SST temperatures (red circles) and T90–100 m temperature section (grey) recorded by the mooring. The temperatures were averaged according to time integrated by each sample and the standard deviations are represented by bars with the same color as the circles. Seasons are exhibited above the x-axis. Shell fluxes from the deployments 1–4 were previously published by Venancio et al. (2016a). (For interpretation of the references to color in this figure legend, the reader is referred to the web version of this article.)

4. Results

4.1. Planktonic foraminifera shell fluxes

Shell fluxes for each of the investigated planktonic foraminifera species for the entire time series are shown in Fig. 2. Shell fluxes ranged from 0 to 489 shells $m^{-2} d^{-1}$ and the values differed among the species. Fluxes of *G. ruber* pink ranged from 0 to 149 shells $m^{-2} d^{-1}$, while *G. ruber* white ranged from 0 to 193 shells $m^{-2} d^{-1}$. In the case of *T. sacculifer* and *O. universa* the values ranged from 0 to 49 shells $m^{-2} d^{-1}$ and from 0 to 63 shells $m^{-2} d^{-1}$, respectively. Finally, the fluxes from *N. dutertrei* and *G. menardii* showed wider ranges with values from 0 to 489 shells $m^{-2} d^{-1}$ and from 0 to 382, respectively.

Similar patterns of shell fluxes were observed during certain deployments. The first of these patterns occurred during the first deployment (November–December 2010), where *N. dutertrei* and *G. menardii* presented very low shell fluxes, while the other species presented flux peaks at the end of November. Shell fluxes from all species were generally higher at the deepest trap (100 m) during this first deployment, which is not necessarily a persistent pattern for the subsequent deployments. Other distinctive patterns occur during the fourth and seventh deployments. During the fourth deployment (December

2011–March 2012) all the species showed flux peaks in December 2011 and lower fluxes until March 2012. During the seventh deployment (September 2013–March 2014), *G. ruber* pink and *G. ruber* white showed comparable flux patterns with a decreasing trend from September to December of 2013 and subsequent increase towards a maximum flux at February of 2014. However, the observed trends for *G. ruber* pink and *G. ruber* white are not statistically significant. The fluxes of the other species, except *G. menardii*, have a statistically significant (p-value < 0.05) decreasing trend, but with no maximum flux occurring during February of 2014. The highest fluxes of *N. dutertrei* and *G. menardii*, 489 and 382 shells $m^{-2} d^{-1}$ respectively, occurred during periods of lower SST values (22–23 °C), while peak fluxes of *G. ruber* white and *G. ruber* pink coincide with higher SST values (> 24 °C).

4.2. Oxygen isotopes

The oxygen isotopic composition ($\delta^{18}O$) of the investigated planktonic foraminifera species showed distinct offsets (Fig. 2). Values for *G. ruber* pink varied from −1.9 to −0.7‰ and from −1.7 to −0.4‰ for *G. ruber* white. In the case of *T. sacculifer* and *O. universa* the values ranged from −1.2 to −0.1‰ and from −1.3 to 0.1‰. The highest values were observed for *N. dutertrei* and *G. menardii*, from −0.8 to 0.4‰ and −1.0 to 0.4‰. Although the ranges of $\delta^{18}O$ values observed for each species were distinct, the amplitude is very similar with values around 1.2 to 1.4‰. It is also noticeable that $\delta^{18}O$ values between different sediment trap-depths showed comparable values, with the exception of *N. dutertrei* and *G. menardii* (Fig. 2), where the $\delta^{18}O$ range from the shallower trap (50 m) was lower than in the simultaneously deployed lower trap (100 m).

4.3. Seasonality of shell flux and temperature

The periodic regression analysis indicates different patterns of intra-annual shell flux variability among the studied species (Table 2; Supporting information Fig. S1). Shell fluxes of *G. ruber* pink, *T. sacculifer*, *O. universa* and *G. menardii* show no significant seasonal component in their flux variability (p > 0.05), allowing us to assume that the fluxes fluctuated randomly around a mean value. Conversely, for *N. dutertrei* and *G. ruber* white, the periodic regression identified a significant (p < 0.01) seasonal component. The fluxes of *G. ruber* white presented higher values during austral summer, with the highest peak at the beginning of the summer, revealing a preference of that species for summer oceanographic conditions in the region. For *N. dutertrei*, the analysis indicates the presence of two cycles during the year, with maxima in spring and autumn. The coefficients of determination for *G. ruber* white (r^2 = 0.46) and *N. dutertrei* (r^2 = 0.39) demonstrate that the periodic model explains a large part of the variance, and the significance remains even when excluding specific years or switching seasons between years (not shown), which confirms the substantial influence of seasonality on the shell fluxes of these species (Fig. 3). Using polynomial regressions instead of a sinusoidal model, to account for alternative shapes of the flux distribution (Supporting information Table S1 and Fig. S5) also reveals no statistically significant results for *O. universa*, *T. sacculifer* and *G. menardii*, but confirms statistically significant results for *G. ruber* white and *N. dutertrei* with peak flux estimated during the same seasons. A general sinusoidal periodic model also indicates significant results for *G. ruber* pink fluxes with the presence of three peaks through the year (Fig. S5). Since we see no mechanism causing this kind of flux variability, we conclude that the flux of this species is virtually constant throughout the year.

As expected, the periodic regression analysis (Table 2; Supporting information Fig. S2) showed a highly significant (p < 0.01) seasonal component in the variation of the AVHRR-SST and the temperatures recorded by the mooring. However, the AVHRR-SST showed a higher coefficient of determination (r^2 = 0.85) than temperatures from different depths of the mooring (0.16 to 0.21), which indicates that a large portion of the subsurface temperature variability in the region is not seasonal or that the satellite temperature values are averaged over an area large enough to alias smaller-scale variability which is preserved in the mooring measurements. It is noteworthy that for AVHRR-SST and for T30–40 m and T40–50 m the analysis revealed the presence of one cycle, while for temperatures at depths below 50 m, we observed the presence of two cycles per year.

Table 2
Results from the periodic regression and ANOVA for the shell fluxes of each planktonic foraminifera species, estimated calcification depths and temperature records.

Data	N° of cycles	Model peak times (DOY)		Amplitude	r^2	p-Value
Flux *G. ruber*	1	349	–	0.2	0.07	0.292
(pink)	2	119	302	0.2	0.14	0.293
Flux *G. ruber*	1	342	–	0.7	0.46	**< 0.001**
(white)	2	132	315	0.2	0.02	0.635
Flux *T. sacculifer*	1	238	–	0.1	0.03	0.908
	2	4	187	0.1	0.02	0.749
Flux *O. universa*	1	272	–	0.2	0.08	0.214
	2	121	303	0.3	0.14	0.265
Flux *G. menardii*	1	261	–	0.2	0.06	0.745
	2	2	185	0.1	0.01	0.083
Flux *N. dutertrei*	1	334	–	0.2	0.10	0.147
	2	119	301	0.4	0.39	**< 0.002**
AVHRR-SST	1	67	–	2.2	0.85	**< 0.001**
	2	134	317	0.2	0.02	**< 0.003**
T30–40	1	146	–	0.8	0.16	**< 0.001**
	2	175	357	0.6	0.05	**< 0.001**
T40–50	1	162	–	0.9	0.21	**< 0.001**
	2	180	363	0.8	0.07	**< 0.001**
T50–60	1	172	–	0.9	0.07	**< 0.001**
	2	3	185	1.0	0.21	**< 0.001**
T60–70	1	173	–	0.8	0.04	**< 0.001**
	2	5	188	1.1	0.20	**< 0.001**
T70–80	1	176	–	0.6	0.02	**< 0.001**
	2	6	189	1.2	0.19	**< 0.001**
T80–90	1	168	–	0.6	0.02	**< 0.001**
	2	6	189	1.1	0.17	**< 0.001**
T90–100	1	169	–	0.5	0.02	**< 0.001**
	2	8	191	1.0	0.15	**< 0.001**
Depth *G. ruber*	1	227	–	14.3	0.44	**< 0.001**
(pink)	2	22	205	10.2	0.18	**0.007**
Depth *G. ruber*	1	227	–	5.7	0.05	0.305
(white)	2	22	204	10.5	0.28	**< 0.01**
Depth *T. sacculifer*	1	256	–	11.5	0.32	0.064
	2	22	205	7.7	0.12	0.221
Depth *O. universa*	1	191	–	4.5	0.07	0.123
	2	10	193	7.8	0.09	0.182
Depth *G. menardii*	1	268	–	1.7	0.03	0.591
	2	25	208	12.6	0.30	**< 0.01**
Depth *N. dutertrei*	1	223	–	2.2	0.04	0.164
	2	21	204	10.1	0.29	**< 0.001**

Statistically significant results shown in bold font.

4.4. Calcification depths and flux-weighted $\delta^{18}O$

The estimated calcification depths revealed consistent differences among planktonic foraminifera species (Fig. 4). *G. ruber* pink and *G. ruber* white (mode 30–40 m) showed shallow calcification depths, followed by *T. sacculifer* and *O. universa* (mode 50–60 m) with more intermediate values, and *N. dutertrei* (mode 60–70 m) together with *G. menardii* (mode 70–80 m) showing the deepest calcification depths. The presence of vertical separation of calcification depths among the species is visible both in the distribution of the absolute values (Fig. 4) as well as when considering the differences in estimated calcification depths of species from the same sediment trap samples (Fig. 5). However, next to the strong inter-specific signal, individual species showed a highly variable range of estimated calcification depths, which is also reflected in a large variability in offsets among the species. For individual species, there seems to be a pattern with the greatest calcification depths

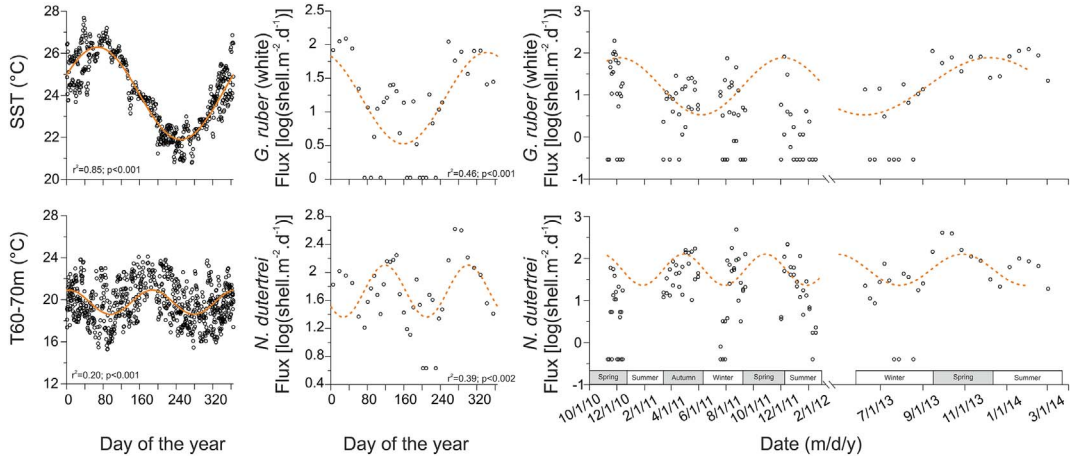

Fig. 3. Periodic-regression results of two temperature sections (AVHRR-SST and T60–70 m) and logarithmic shell fluxes of *G. ruber* (white) and *N. dutertrei*. Coefficients of determination values and p-values are given for each dataset. The lines in orange represent the models for the temperatures (solid lines) and for the shell fluxes (dashed lines). In the left panels the time is represented as days of the year and the shell fluxes are derived from the deployments 2, 6 and 7, while temperatures are daily records for the entire time series. In the right panels are the logarithmic shell fluxes of *G. ruber* (white) and *N. dutertrei* for the entire time series plotted with the model (orange dashed line) produced by the periodic regression. Seasons are exhibited above the x-axis of the right panel. (For interpretation of the references to color in this figure legend, the reader is referred to the web version of this article.)

(> 50 m) more frequently observed in summer and winter. Indeed, periodic regression of the estimated calcification depths pooled for each species across all traps and sampling intervals (Table 2) indicates significant cyclic component in the variation of calcification depth in four out of the six analyzed species (Fig. 4). The periodic regression explains about one third of the variance in the calcification depth data for those four species (*G. ruber* pink and white, *G. menardii* and *N. dutertrei*) and implies an objectively defined maximum calcification depth values in July (DOY 204–227) for these four species and also in January (DOY 21–25) for three of the species (*G. ruber* white, *G. menardii* and *N. dutretrei*) (Fig. 4, Table 2). These are the times of the year (DOY 21–25 and 204–227) with deep (≈ 100 m) mixed layer (Fig. S3), which means the inferred calcification depth would be deeper without any change in habitat preference of those species. For *O. universa* and *T. sacculifer*, the variability in estimated calcification depths does not appear to have a periodic component.

When calculating the calcification depth, we noted that 4% of the oxygen isotopic values exceed the range of possible predicted $\delta^{18}O$ ($\delta^{18}O_{predicted}$). This indicates that these foraminifera may have calcified in another (warmer) region, being subsequently transported to our site. This discrepancy is not observed for the deeper end of estimated calcification depths. Here, all of the observed $\delta^{18}O$ could have resulted from calcification above the sediment trap during the sampling interval. This is not to say that we can exclude that the calcification of some specimens occurred below 100 m and these specimens were still captured by the trap, because they ascended in the water column after the calcification due to water mass mixing or vertical migration. However, the data can be explained without requiring the existence of these mechanisms.

To obtain an estimate of the stable isotopic composition of sedimentary foraminifera that would be deposited below the sediment trap, we calculated flux-weighted annual mean $\delta^{18}O$ for the studied species. Because the seasonal component in shell fluxes was weak, the flux-weighted $\delta^{18}O$ values should mainly reflect specific calcification depths (Table 3). In fact, the effect of flux weighting on the annual mean $\delta^{18}O$ was negligible (Table 3). The lowest value of flux-weighted mean annual $\delta^{18}O$ (− 1.29‰) was shown by *G. ruber* pink, in line with the inferred shallower calcification depth for this species, while *N. dutertrei* showed the highest value (− 0.26‰), in line with its deepest estimated calcification depth. Flux-weighted $\delta^{18}O$ values for *T. sacculifer* and *O. universa* were − 0.67 and − 0.56‰, in line with the similar calcification depth estimates for these species. This points to a comparable habitat for *T. sacculifer* and *O. universa* in the studied region.

5. Discussion

Since the focus of this work is to provide information relevant for paleoceanographic studies using foraminifera-based proxies in the western South Atlantic, we begin by considering the main factors that can influence the interpretations of paleo-records in this region. We show the depth ranges in which each species calcify and how they may change seasonally (Section 5.2), but we also present an evaluation of the magnitude and timing of the seasonal component in the foraminifera fluxes (Section 5.1). Insights about both factors, seasonality of the shell fluxes and calcification depths, are necessary since a species may vary its abundance in the water seasonally, independently from its habitat, resulting in a mixed signal in the sediment. A consideration of both the seasonal and vertical habitat of the studied species allowed us to predict the isotopic signal in surface sediments and show the potential of a multi-species approach for reconstructing past changes in the water column structure (Section 5.3).

5.1. Seasonal fluxes

As pointed out by Jonkers and Kucera (2015), the seasonal component modulating shell fluxes in planktonic foraminifera is species-specific and varies spatially. For the six species analyzed in this study, the seasonal component in the flux data was significant only for *G. ruber* white and *N. dutertrei* (Table 2; Supporting information Fig. S1). This observation indicates that most of the warm-water species analyzed here (*G. ruber* pink, *T. sacculifer*, *O. universa*, *G. menardii*) show no seasonal bias in their flux and their sedimentation should reflect mean annual conditions. This is in line with the inferred decreasing amplitude of seasonal flux peaks in warm-water species towards the tropics (Jonkers and Kucera, 2015). Even in the two species that showed a seasonal variation in their shell flux, the amplitude of the inferred seasonality is small and has little effect on the flux-weighted $\delta^{18}O$.

Because of the observed temperature dependency of flux seasonality in planktonic foraminifera (Jonkers and Kucera, 2015), a comparison with previous observations must be restricted to sediment traps from similar temperature settings. In this respect, a sediment trap record located at 11°S in western Atlantic (Žarić et al., 2005) also shows no significant seasonal component for any of the studied species, and nearby sediment trap record at 7°S (Žarić et al., 2005), shows seasonal components in the flux of *G. ruber* pink and *T. sacculifer*, but with a very low amplitude. These observations confirm that in the warm-water region of the western tropical Atlantic, shell fluxes of planktonic

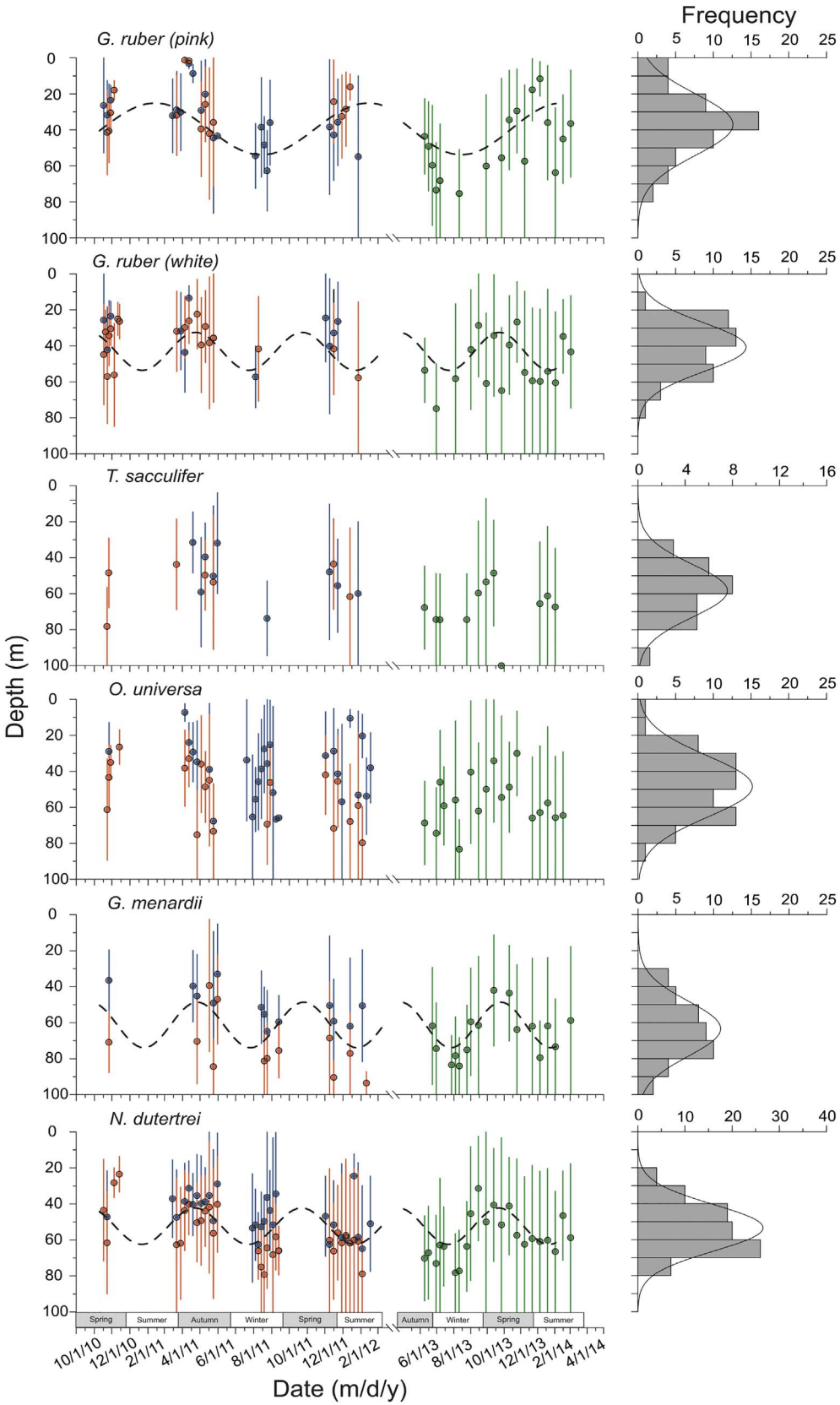

Fig. 4. Calcification depths estimated for each planktonic foraminifera species for the entire time series. Maximum and minimum calcification depths are represented by the lines and the mean values are represented by circles. Colors represent the different trap depths 50 m (blue), 100 m (orange) and 75 m (green). The right panels are histograms displaying the distribution of the mean values (grey bars) of calcification depths with the Gaussian distribution (black line). Seasonal component of the mean calcification depths was analyzed by periodic regression and the black dashed lines represent the models that were significant. Seasons are exhibited above the x-axis. (For interpretation of the references to color in this figure legend, the reader is referred to the web version of this article.)

foraminifera show only weak seasonality.

For the species in which we observe a significant seasonal component (*G. ruber* white and *N. dutertrei*) one may ask which environmental conditions caused this preference towards a certain period or season (Fig. 3). For *G. ruber* white, we observed higher fluxes during summer (Fig. 3). This pattern cannot be solely attributed to the temperature preference of *G. ruber* white, because the species *G. ruber* pink and *T. sacculifer* show an equivalent degree of affinity towards warmer

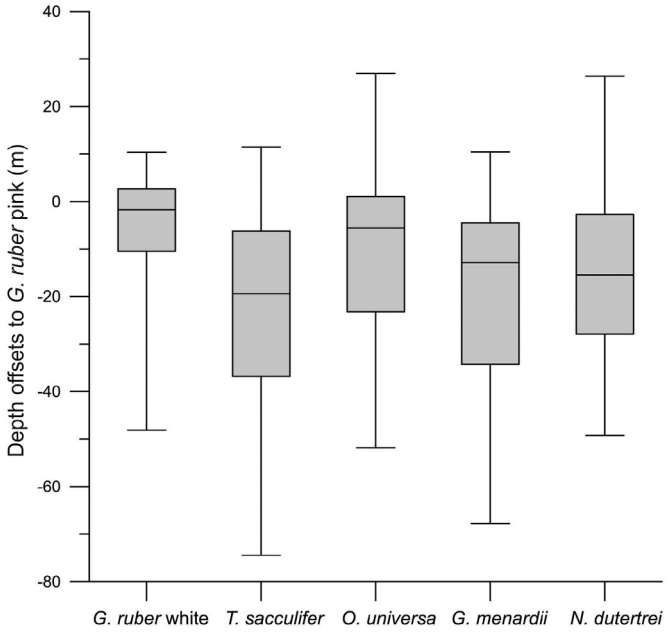

Fig. 5. Box-and-whisker plots of the depth offsets of mean calcification depths of the investigated planktonic foraminifera species in relation to *G. ruber* pink calcification depths. The interspecific comparison was done only for calcification depths estimated in the same sample.

temperatures (Kucera, 2007), but none of them peaks in summer. An affinity to oligotrophic conditions cannot explain the summer peak of *G. ruber* white either, because other tropical surface-dwelling species appear to be even better adapted to such conditions (Siccha et al., 2009). Instead we hypothesize that the detection of the seasonal cycle in the flux of *G. ruber* white reflects a combination of high SST and deep mixed layer during summer (Table 2; Supporting information Fig. S2). The fact that *G. ruber* pink does not show an increase in flux during these summer conditions is coherent, since previous studies suggested the dominance of *G. ruber* white over *G. ruber* pink when the mixed layer deepens (Ufkes et al., 1998; Sousa et al., 2014). In addition, the changes in habitat of *G. ruber* white are similar to the dynamics of the base of the mixed layer in the region (Fig. 4; Table 2), unlike the other surface-dwelling species (*G. ruber* pink, *T. sacculifer* and *O. universa*), showing that this species is more sensitive to mixed layer changes and calcifies deeper during times when the mixed layer deepens.

The flux of *N. dutertrei* shows two peaks coinciding with periods of shoaling of the 18 °C isotherm in our study area (Fig. 3; Supporting information Fig. S3). Thus, it seems that *N. dutertrei* abundance increases when the thermocline is shallower, which is in agreement with previous findings, relating this species to thermocline dynamics (Fairbanks and Wiebe, 1980; Ravelo et al., 1990). Shoaling of the thermocline implies shoaling of the nutricline, which could stimulate population growth of the species either directly, by providing more nutrients to its symbionts or indirectly, by stimulating phytoplankton growth at depth. This hypothesis is supported by the consistently deepest estimated calcification depth for *N. dutertrei* (Figs. 4, 5). The fact that the same pattern is not observed for *G. menardii* can be explained by lower abundances of this species, resulting in a more "noisy" flux pattern (Fig. 2, Supporting information Fig. S1).

Considering the coefficients of determination of the periodic regression models, it is important to bear in mind that even for those species in which we observe a significant seasonal component, most of the flux variability cannot be explained in this way. As pointed out by Jonkers and Kucera (2015), this fact may be due to processes occurring at frequencies different from the annual cycle, such as lunar cycles, long-term trends or even non-periodic and random signals.

5.2. Calcification depths

The knowledge of the calcification depth of planktonic foraminifera species is indispensable in order to understand the signals derived from geochemical proxies recorded in their calcite. Because of discontinuous growth, calcification depth in planktonic foraminifera is not equivalent to habitat depth. Habitat depth is an ecological concept, describing the depth range where a population of a given species will be found. In contrast, calcification depth reflects the water depth at which most of the calcite of the shell has been precipitated and hence where the isotopic and trace-elemental signature of the shell is acquired. Habitat depth can be inferred directly from stratified plankton net samples. In contrast, calcification depth has to be inferred indirectly by comparing shell composition with vertical profiles of water properties and inferring at what depth the shell was most likely to be produced. This procedure incurs large uncertainties, and results from earlier studies are inconclusive as to the exact values of calcification depths and their regional (and temporal) stability (Cléroux et al., 2013; Farmer et al., 2007; Jonkers et al., 2010; Ravelo and Fairbanks, 1992; Sagawa et al., 2013; Simstich et al., 2003; Steph et al., 2009; Tedesco et al., 2007; Wejnert et al., 2013; Asahi et al., 2015).

Our study indicates species-specific typical calcification depths, which are variable in absolute values, but consistent in their order among the species. We observe that both varieties of *G. ruber* show shallowest calcification depths, with mode values around 30 to 40 m (Fig. 4). Both species showed a seasonal component in the estimated calcification depth with deeper calcification during winter (*G. ruber* white also in summer), reflecting deepening of the mixed layer during this period, which necessarily leads to greater estimates of calcification depth. This observation implies that both species are consistently

Table 3
Species-specific estimations of $\delta^{18}O$ flux-weighted, annual mean $\delta^{18}O$, core tops $\delta^{18}O$, calcification depth, seasonal component in calcification depth and seasonal component in shell fluxes.

Species	$\delta^{18}O$ Flux-weighted (‰)	Annual mean $\delta^{18}O$ (‰)	Core tops $\delta^{18}O$ (‰)*	Calcification depth (m)	Seasonal depth (season; peak)	Model flux peak (season; peak)
G. ruber (*pink*)	− 1.29	− 1.27	− 0.75 (± 0.14)[a]; − 1.16[c]	30–40	Winter (DOY 227)	–
G. ruber (*white*)	− 1.06	− 1.08	− 0.89[b]; − 0.99[c]	30–40	Summer/winter (DOY 23; 205)	Summer (DOY 342)
T. sacculifer	− 0.67	− 0.68	− 0.54 (± 0.14)[a]; − 0.55[c]	50–60	–	–
O. universa	− 0.56	− 0.56	No data	≈ 50	–	–
G. menardii	− 0.30	− 0.37	0.06 (± 0.18)[a]	70–80	Summer/winter (DOY 25; 208)	–
N. dutertrei	− 0.26	− 0.25	0.13 (± 0.16)[a]	60–70	Summer/winter (DOY 21; 204)	Fall/spring (DOY 119; 301)

* a: BCCF10-01 in Venancio et al. (2016b) – 100-yr mean values and standard deviations, recent age confirmed by age model based on ^{210}Pb excess; b: CF10-01 in Lessa et al. (2016) – top centimeter with an age of 1030 yr confirmed by ^{14}C dating; c: GeoB3207-2 in Chiessi et al. (2007) – uppermost centimeters with recent age confirmed by the presence of stained benthic foraminifera.

calcifying in the mixed layer, irrespective of its thickness. Shallow (mixed-layer) calcification depths for *G. ruber* white of 20 to 40 m were also estimated by Babila et al. (2014) using sediment traps from the Sargasso Sea. In sediment traps located in Cariaco Basin, calcification depths for *G. ruber* pink were also mostly in the same depth range, albeit with some deeper estimations up to 100 m during specific periods in the time series (Tedesco et al., 2007; Wejnert et al., 2013). Studies using surface sediments from the tropical Atlantic also pointed to a similar range of calcification depth for *G. ruber* (Farmer et al., 2007; Steph et al., 2009). Collectively, our findings and the literature data reviewed above suggest that despite temporal and regional variability in the oceanographic conditions in their habitat, the calcification of both varieties of *G. ruber* occurs within the mixed layer.

Estimated calcification depths for *O. universa* and *T. sacculifer* yielded slightly deeper values (50–60 m) than *G. ruber* (pink and white) (Figs. 4 and 5). Thus, the calcification habitat of these species must extend below the mixed layer. This conclusion is supported by the observation that these species did not show a significant seasonal component in their calcification depths (Table 2), which indicates that their depth habitat is not strictly linked to the mixed layer dynamics. A study in the western tropical Indian Ocean also observed similar calcification depths between *O. universa* and *T. sacculifer*, characterizing both as deeper mixed layer species (Birch et al., 2013). Previous studies also pointed to deeper calcification of *O. universa* and *T. sacculifer* in comparison to *G. ruber* (Steph et al., 2009; Tedesco et al., 2007; Wejnert et al., 2013). In contrast, Farmer et al. (2007) found no differences in calcification depths among these three species, although they also noted a wider calcification depth range for *O. universa*.

For the deep-dwelling species (*N. dutertrei* and *G. menardii*), the estimated calcification depths are also consistently deeper than those of *G. ruber* (Fig. 5), ranging mostly below 50 m (Fig. 4). Both species show a seasonal component in their calcification depths (Table 2), with greater calcification depths during summer and winter when the mixed layer deepens. This is consistent with tracking of a subsurface habitat throughout the year. Indeed, the estimated calcification depths for *N. dutertrei* have a mode in the interval between 60 and 70 m. This value is in agreement with the reported thermocline depth or the 18 °C isotherm for the region (Valentin, 2001; Albuquerque et al., 2014) and with our temperature records (Supporting information Fig. S3), which show the presence of the 18 °C isotherm between 60 and 80 m, mainly during spring and autumn. An upper thermocline calcification depth for this species is in agreement with previous studies (Farmer et al., 2007; Steph et al., 2009), including the estimates from Sagawa et al. (2013) who estimated a 25–35 m calcification depth for *N. dutertrei* in the western North Pacific in summer, where the seasonal mixed layer is shallow. In the Cariaco Basin (Tedesco et al., 2007; Wejnert et al., 2013), the calcification habitat of this species also corresponds to the uppermost thermocline and it appears to follow the seasonal upwelling pattern with deep calcification coinciding with the cessation of upwelling in fall. Although the number of observations on *G. menardii* is lower in our study due to lower abundance, it shows similar behavior as *N. dutertrei* in all respects, which is consistent with observations from Cariaco Basin (Tedesco et al., 2007; Wejnert et al., 2013).

Because of the observed high level of consistency between the measured $\delta^{18}O$ values in the investigated foraminifera species and predicted values for the water column above the sediment traps, we can exclude expatriation (Berger, 1970) as a significant process affecting the foraminiferal flux. Only 4% of $\delta^{18}O$ values were out of range of possible species-specific $\delta^{18}O_{predicted}$ curves. All of these values exceeded predictions towards the warmer end, but with different probabilities between the analyzed species. This was more frequent for *G. ruber* white, *G. ruber* pink and *O. universa*, which showed 9.3, 5.4 and 6.2% of $\delta^{18}O$ values out of range, while this was observed in $< 3\%$ of the cases for the other species. A possible explanation for the observed discrepancies is that the chosen species-specific equations are not adequate. However, these discrepancies remain even when changing the paleotemperature equations (not shown). Thus, some of the analyzed foraminifera appear to have calcified under warmer conditions outside of the studied area and were then transported to the sediment traps. This is a reasonable assumption, since our mooring is located over the southeastern continental shelf, which can be influenced by intense lateral transport. Therefore, specimens with a distinct oxygen isotopic signature may have been passively transported to our region by lateral advection, but their flux appears to have been overwhelmed by local production.

Finally, we consider the bias that may arise from the fact that our $\delta^{18}O$ measurements could not be carried out in a narrow size range. In this scenario, part of the intra-specific $\delta^{18}O$ signal may be due to the size variation of the analyzed specimens. Indeed, Ezard et al. (2015) using a statistical model approach, suggest a size dependency in $\delta^{18}O$ for species analyzed in this study. However, the trend arises from values recorded mainly in small specimens and no clear $\delta^{18}O$ trend with size can be identified in their raw data compilation for the analyzed species within the size range used here for the isotopic measurements. Furthermore, Birch et al. (2013) in a study in the western Indian Ocean analyzed multi-species through different size ranges and although a significant size-dependent effect was observed for the $\delta^{13}C$, the authors concluded that no significant correlation was observed between the size of the test and the $\delta^{18}O$ composition of *G. ruber*, *T. sacculifer* and *O. universa*. These observations suggest that although an influence of the test size on the $\delta^{18}O$ may exist, it is unlikely to have accounted for a substantial part of the variance in the $\delta^{18}O$ signal of the analyzed species. The existence of a stronger dependency of $\delta^{13}C$ on size is also the reason why $\delta^{13}C$ variation is not being considered in this study.

5.3. Paleoceanographic implications

The southwestern Atlantic has been the focus of recent paleoceanographic studies, with most of these reconstructions using planktonic foraminifera assemblages or the geochemical composition of their shells in order to reconstruct past surface water conditions (Chiessi et al., 2014; Chiessi et al., 2015; Lessa et al., 2016). For instance, these studies used the geochemical composition of the shells of *G. ruber* (white) (Chiessi et al., 2014; Lessa et al., 2016) without considering the possibility that this species might not be recording mean annual conditions or that the recorded signal might come from deeper layers. Our results for *G. ruber* (white) show that the fluxes of this species increase during summer conditions and that their calcification depths are variable and linked to the dynamics of the mixed layer, although the mean signal is linked to the depths of 30–40 m. Thus, our findings can provide important constraints on the temporal and vertical distribution of the planktonic foraminifera species fluxes and the resulting $\delta^{18}O$ signatures in their shells, which may help improve paleoceanographic interpretations for the region. Moreover, with this information it becomes easier to evaluate which species are more suitable for paleoceanographic reconstructions in the area. To this end, we first compared the $\delta^{18}O$ signature exported by the different species to the sediment (flux-weighted mean annual $\delta^{18}O$) with $\delta^{18}O$ values observed in recent sediments from the same area. We observe that for all species, the flux-weighted mean annual $\delta^{18}O$ preserve the same species offsets, but the values are lower than the $\delta^{18}O$ values measured in recent sediments (Table 3, Fig. 6), except *O. universa* for which no data is available from recent sediments.

The sedimentary values could be higher for several reasons. First, sediment samples represent multi-annual averages and their mean isotopic signal is therefore skewed towards years with higher flux. However, as the species fluxes showed little or no seasonality in our region (Fig. 3; Supporting information), this process is unlikely to account for the large offsets we observe (up to 0.4‰; Table 3). Alternatively, the difference could reflect recent warming in the region, which is not reflected in the sediment signature because of temporal averaging. This is not unreasonable, because the observed $\delta^{18}O$ offset

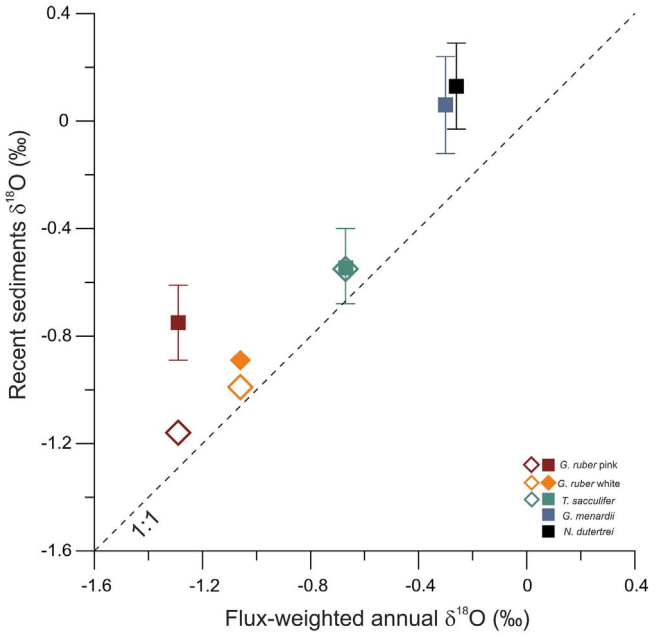

Fig. 6. Offset between flux-weighted mean annual $\delta^{18}O$ and $\delta^{18}O$ values from recent sediments provided by several studies for each of the investigated planktonic foraminifera species, except *O. universa*. Open diamonds represent the offsets using the core top $\delta^{18}O$ values derived from GeoB3207-2 (Chiessi et al., 2007). Diamonds represent core top $\delta^{18}O$ values derived from CF10-01 (Lessa et al., 2016). Squares with standard deviations represent a 100-yr average of $\delta^{18}O$ values derived from the box-core BCCF10-01 (Venancio et al., 2016b).

corresponds to $< 2\,^{\circ}C$. Finally, the offset may be due to the fact that planktonic foraminifera form a secondary layer of calcite at the end of their life cycle, which results in higher values of $\delta^{18}O$ (Bé, 1980; Erez and Honjo, 1981). Because of their shallow position at 50–100 m, our traps may have collected not only dead specimens (empty shells) but also live specimens that would have continued growing if they had not entered the trap. Therefore, there is a higher probability to find individuals which have acquired the heavier $\delta^{18}O$ signal associated with secondary calcite in the sediments than in our traps.

Since the sediment and the trap have different mechanisms of particle delivery, the difference could also reflect lateral transport of shells along the sea floor. An intense along-shelf and cross-shelf transport could entrain foraminifera that were originally deposited shallower, closer to coast. Due to the presence of upwelling systems along the southeastern Brazilian coast, these shells could have acquired a heavier $\delta^{18}O$ signature due to lower surface (or subsurface) temperatures in these regions, being subsequently transported to the sediments below our mooring line. However, we observe that $\delta^{18}O$ differences between species are still in agreement in both set of samples (traps and sediments), which means that the vertical differences in calcification depths were kept in the fossil record. We also note that planktonic foraminifera are known to avoid shallow waters (Schmuker and Schiebel, 2002) and the flux of specimens that would calcify over shelf areas substantially shallower and thus far away from the traps was likely small. Summarizing, we conclude that the main pattern of interspecies isotopic offsets is preserved in sediment assemblages.

Since *G. ruber* pink exhibits the shallowest calcification depth with relatively constant annual fluxes, it would be the best species to characterize surface-ocean conditions in the southwestern Atlantic. Moreover, this species is very abundant in surface sediments in the area (Lessa et al., 2014). In contrast, *N. dutertrei* appears to calcify within the seasonal thermocline and it consistently tracks this habitat throughout the year (Fig. 4). Its fluxes also appear to be influenced by the depth of the thermocline, but the amplitude of the signal is low and does not affect the flux-weighted annual mean (Table 3). Consequently, *N. dutertrei* $\delta^{18}O$ could be used to reconstruct the temperature of the seasonal thermocline. Although *G. menardii* could also be used to reconstruct the thermocline conditions, this species has low abundances in the trap and sediment samples in the area, and is absent during glacial periods in the cores located in the Brazilian margin (Vicalvi, 1997; Portilho-Ramos et al., 2015), making it difficult to use the $\delta^{18}O$ of *G. menardii* for paleoceanographic reconstructions on glacial-interglacial timescales.

The difference between shell geochemistry of *G. ruber* pink and *N. dutertrei*, for example the $\Delta\delta^{18}O$ of these species, should thus be a proxy for stratification. The use of such a proxy for paleoceanographic reconstructions was already proposed in sediment traps studies from the Cariaco Basin (Tedesco et al., 2007; Wejnert et al., 2013). In order to validate this approach in our region, we compared the $\Delta\delta^{18}O$ between *N. dutertrei* and *G. ruber* pink with temperature difference between depths where the specimens calcified (Fig. 7). Although *G. ruber* pink calcifies mostly around 30–40 m, we used the temperature difference from the surface (SST) to the thermocline (60–70 m), since *G. ruber* pink may calcify at shallower depths. For the thermocline layer we used the temperatures extracted from 60 to 70 m, which coincide with the mean calcification depth of *N. dutertrei*, and represent the same seasonal

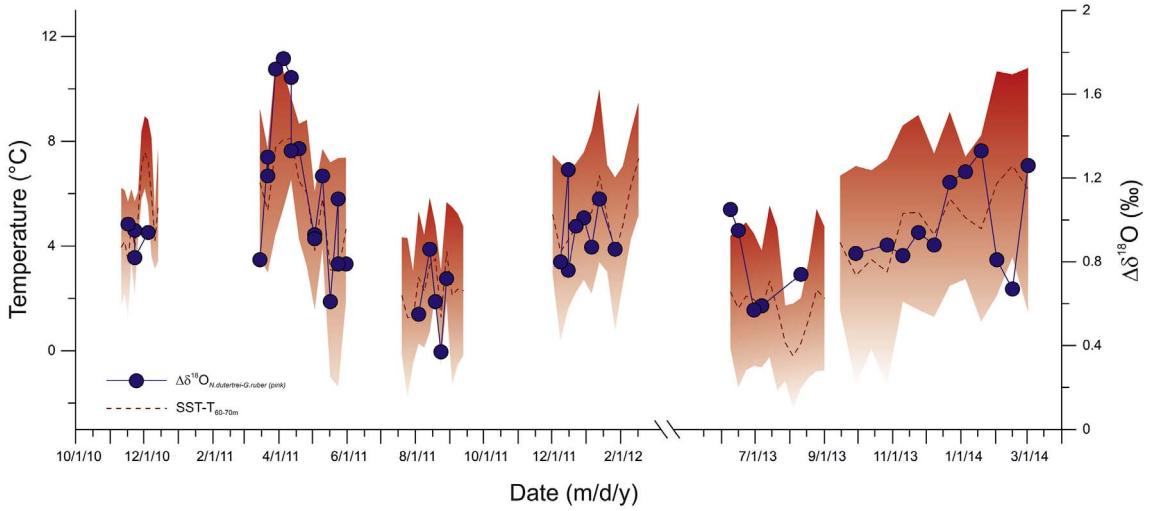

Fig. 7. Temperature difference between AVHRR-SST and T60–70 m plotted with the oxygen isotopic difference ($\Delta\delta^{18}O$) between *G. ruber* pink and *N. dutertrei*. Temperature difference is represented by the red dashed line, with the errors estimated by error propagation represented by the shades of red. The ($\Delta\delta^{18}O$) between *G. ruber* pink and *N. dutertrei* is represented by the blue line and circles. (For interpretation of the references to color in this figure legend, the reader is referred to the web version of this article.)

temperature pattern of the temperatures recorded below 50 m (Table 2; Supporting information).

The estimated calcification depths of *G. ruber* pink were mostly around 30–40 m, with the presence of a seasonal cycle in calcification depth, indicating calcification within the mixed layer, while estimated calcification depths for *N. dutertrei* were mostly around 60–70, also with a significant seasonal component, but with calcification corresponding to the uppermost thermocline (Fig. 4). Since the annually averaged sedimentary signal cannot resolve such seasonal habitat migration it would instead record a flux-weighted mean offset in calcification depths between the species. We observed that the annual mean flux weighted $\Delta\delta^{18}O$ offset between the species is 1.03‰, which corresponds well to the annual mean difference in predicted $\delta^{18}O$ of 1.08‰ between 30 and 40 m and 60–70 m.

In summary, we show that planktonic foraminifera species in the studied area show consistent isotopic offsets reflecting mainly their preferred habitats and that this signal is preserved in the sediment and only minimally modified by secondary calcite formation or expatriation. Therefore, stratification is captured by interspecific oxygen isotopic signatures. The apparent ability to reconstruct stratification in the studied region could provide valuable information regarding the strength of the Brazil Current (Belem et al., 2013) and the state of the nearby upwelling systems (Cordeiro et al., 2014; Souto et al., 2011; Lessa et al., 2016). This exemplifies the potential of species-specific calcification depth estimations and highlights the importance of local assessments using continuous high-resolution records with co-registered hydrography. However, there is still a need for longer and continuous time series, as well as better estimates generated by species-specific calibrations in order to reduce uncertainties and improve our knowledge about the calcification depths of planktonic foraminifera species. Nevertheless, our results provide an initial basis for future regional foraminifera-based proxy development, since it shows to what water depth (or depth range) the chemical composition of each planktonic foraminifera species should be attributed, thus indicating to what water depth must a target environmental parameter be calibrated when developing a proxy using one of the species here analyzed.

6. Conclusions

Based on our mooring records we estimated the influence of the seasonal component in the shell fluxes of six planktonic foraminifera species and in their calcification depth ranges in the southwestern Atlantic. Our main observations revealed the following:

- The majority of the warm-water species analyzed here (*G. ruber* pink, *T. sacculifer*, *O. universa*, *G. menardii*) exhibit no significant seasonal component in their shell fluxes and most likely reflect mean annual conditions. Only the fluxes of *G. ruber* white and *N. dutertrei* exhibit a significant seasonal component, with *G. ruber* white showing a single flux peak in austral summer, while *N. dutertrei* exhibits two flux peaks in spring and autumn, but the amplitude of the inferred flux seasonality was small.
- Estimated calcification depths indicate species-specific mean calcification depth, albeit overprinted by a considerable variability throughout the year. The estimated calcification depths for *N. dutertrei* (mode 60–70 m) and *G. menardii* (mode 70–80 m) appear to track the depth of the thermocline in the region, whereas the calcification depths of *G. ruber* pink and white correspond to conditions in the mixed layer. The calcification habitat of *O. universa* and *T. sacculifer* extends below the mixed layer and these species show no systematic seasonal variation in their calcification depth.
- Isotopic offsets among the species in sediment samples are mainly due to different calcification depths. The lower values in oxygen isotopic composition in sediment samples (up to 0.4‰) relative to the trap samples can be explained by the presence of specimens, which added a secondary layer of calcite at the end of their life cycle.
- Although longer and continuous time series are still needed, our calcification depth estimations and assessments of the influence of seasonality provide an initial basis for paleoceanographic interpretations in the study area and allow further studies to reconstruct water column parameters at specific depth ranges using multi-species approach. For example, the $\Delta\delta^{18}O$ between surface species (best represented by *G. ruber* pink) and thermocline species (best represented by *N. dutertrei*) can be used for evaluating stratification in the southwestern Atlantic.

Acknowledgments

This study was financially supported by the Geochemistry Network from Petrobras/National Petroleum Agency (ANP) of Brazil (Grant 0050.004388.08.9). A.L.S. Albuquerque is senior scholar from CNPq (National Council for the Development of Science and Technology, Brazil, Grant 306385/2013-9). The CNPq also financially supported Igor Venancio with a scholarship from the CsF ("Ciencia sem Fronteiras") project (Grant 248819/2013-5). This work was also funded through the DFG Research Center/Cluster of Excellence "The Ocean in the Earth System".

Appendix A. Supplementary data

Supplementary data to this article can be found online at http://dx.doi.org/10.1016/j.marmicro.2017.08.006.

References

Albuquerque, A.L.S., Belém, A.L., Zuluaga, F.J.B., Cordeiro, L.G.M., Mendoza, U., Knoppers, B.a., Gurgel, M.H.C., Meyers, P.a., Capilla, R., 2014. Particle fluxes and bulk geochemical characterization of the Cabo Frio Upwelling System in southeastern Brazil: sediment trap experiments between spring 2010 and summer 2012. An. Acad. Bras. Cienc. 86, 601–619. http://dx.doi.org/10.1590/0001-37652014107212.

Al-Sabouni, N., Kucera, M., Schmidt, D.N., 2007. Vertical niche separation control of diversity and size disparity in planktonic foraminifera. Mar. Micropaleontol. 63, 75–90. http://dx.doi.org/10.1016/j.marmicro.2006.11.002.

Asahi, H., Okazaki, Y., Ikehara, M., Khim, B.K., Nam, S. Il, Takahashi, K., 2015. Seasonal variability of $\delta^{18}O$ and $\delta^{13}C$ of planktic foraminifera in the Bering Sea and central subarctic Pacific during 1990–2000. Paleoceanography 30, 1328–1346. http://dx.doi.org/10.1002/2015PA002801.

Aurahs, R., Treis, Y., Darling, K., Kucera, M., 2011. A revised taxonomic and phylogenetic concept for the planktonic foraminifer species *Globigerinoides ruber* based on molecular and morphometric evidence. Mar. Micropaleontol. 79, 1–14. http://dx.doi.org/10.1016/j.marmicro.2010.12.001.

Babila, T.L., Rosenthal, Y., Conte, M.H., 2014. Evaluation of the biogeochemical controls on B/Ca of *Globigerinoides ruber* white from the Oceanic Flux Program, Bermuda. Earth Planet. Sci. Lett. 404, 67–76. http://dx.doi.org/10.1016/j.epsl.2014.05.053.

Bé, A.W.H., 1980. Gametogenic calcification in a spinose planktonic foraminifer, *Globigerinoides sacculifer* (Brady). Mar. Micropaleontol. 5 (3), 283–310. http://dx.doi.org/10.1016/0377-8398(80)90014-6.

Belem, A.L., Castelao, R.M., Albuquerque, A.L., 2013. Controls of subsurface temperature variability in a western boundary upwelling system. Geophys. Res. Lett. 40, 1362–1366. http://dx.doi.org/10.1002/grl.50297.

Bell, K.N.I., Cowley, P.D., Whitfield, A.K., 2001. Seasonality in frequency of marine access to an intermittently open estuary: implications for recruitment strategies. Estuar. Coast. Shelf Sci. 52, 327–337. http://dx.doi.org/10.1006/ecss.2000.0709.

Bemis, B.E., Spero, H.J., Bijma, J., Lea, D.W., 1998. Reevaluation of the oxygen isotopic composition of planktonic foraminifera: experimental results and revised paleotemperature equations. Paleoceanography 13, 150–160. http://dx.doi.org/10.1029/98PA00070.

Bemis, B.E., Spero, H.J., Thunell, R.C., 2002. Using species-specic paleotemperature equations with foraminifera: a case study in the Southern California Bight. Mar. Micropaleontol. 46, 405–430.

Berger, W., 1970. Planktonic foraminifera: differential production and expatriation off Baja California. Limnol. Oceanogr. 15, 183–204. http://dx.doi.org/10.4319/lo.1970.15.2.0183.

Birch, H., Coxall, H.K., Pearson, P.N., Kroon, D., O'Regan, M., 2013. Planktonic foraminifera stable isotopes and water column structure: disentangling ecological signals. Mar. Micropaleontol. 101, 127–145. http://dx.doi.org/10.1016/j.marmicro.2013.02.002.

Bouvier-Soumagnac, Y., Duplessy, J.C., 1985. Carbon and oxygen isotopic composition of planktonic foraminifera from laboratory culture, plankton tows and recent sediment: implications for the reconstruction of paleoclimatic conditions and of the global carbon cycle. J. Foraminifer. Res. 15 (4), 302–320.

Brandini, F.P., 1990. Hydrography and characteristics of the phytoplankton in shelf and oceanic waters off southeastern Brazil during winter (July/August 1982) and summer (February/March 1984). Hydrobiologia 196, 111–148. http://dx.doi.org/10.1007/BF00006105.

deBruyn, a.M.H., Meeuwig, J.J., 2001. Detecting lunar cycles in marine ecology: periodic regression versus categorical ANOVA. Mar. Ecol. Prog. Ser. 214, 307–310. http://dx.doi.org/10.3354/meps214307.

Calado, L., da Silveira, I.C.A., Gangopadhyay, A., de Castro, B.M., 2010. Eddy-induced upwelling off Cape São Tomé (22°S, Brazil). Cont. Shelf Res. 30, 1181–1188. http://dx.doi.org/10.1016/j.csr.2010.03.007.

Campos, E.J.D., Velhote, D., Area, T.S., 2000. Shelf break upwelling driven by Brazil Current cyclonic meanders. Geophys. Res. Lett. 27, 751–754.

Castelao, R.M., 2012. Sea surface temperature and wind stress curl variability near a cape. J. Phys. Oceanogr. 42, 2073–2087. http://dx.doi.org/10.1175/JPO-D-11-0224.1.

Castelao, R.M., Barth, J.a., 2006. Upwelling around Cabo Frio, Brazil: the importance of wind stress curl. Geophys. Res. Lett. 33, L03602. http://dx.doi.org/10.1029/2005GL025182.

Castro, B.M., 2014. Summer/winter stratification variability in the central part of the South Brazil Bight. Cont. Shelf Res. 89, 15–23. http://dx.doi.org/10.1016/j.csr.2013.12.002.

Cerda, C., Castro, B.M., 2014. Hydrographic climatology of South Brazil Bight shelf waters between Sao Sebastiao (24°S) and Cabo Sao Tome (22°S). Cont. Shelf Res. 89, 5–14. http://dx.doi.org/10.1016/j.csr.2013.11.003.

Chiessi, C.M., Ulrich, S., Mulitza, S., Pätzold, J., Wefer, G., 2007. Signature of the Brazil-Malvinas Confluence (Argentine Basin) in the isotopic composition of planktonic foraminifera from surface sediments. Mar. Micropaleontol. 64, 52–66. http://dx.doi.org/10.1016/j.marmicro.2007.02.002.

Chiessi, C.M., Mulitza, S., Groeneveld, J., Silva, J.B., Campos, M.C., Gurgel, M.H.C., 2014. Variability of the Brazil Current during the late Holocene. Palaeogeogr. Palaeoclimatol. Palaeoecol. 415, 28–36. http://dx.doi.org/10.1016/j.palaeo.2013.12.005.

Chiessi, C.M., Mulitza, S., Mollenhauer, G., Silva, J.B., Groeneveld, J., Prange, M., 2015. Thermal evolution of the western South Atlantic and the adjacent continent during termination 1. Clim. Past 11, 915–929. http://dx.doi.org/10.5194/cp-11-915-2015.

Cléroux, C., DeMenocal, P., Arbuszewski, J., Linsley, B., 2013. Reconstructing the upper water column thermal structure in the Atlantic Ocean. Paleoceanography 28, 503–516. http://dx.doi.org/10.1002/palo.20050.

Cordeiro, L.G.M.S., Belem, A.L., Bouloubassi, I., Rangel, B., Sifeddine, A., Capilla, R., Albuquerque, A.L.S., 2014. Reconstruction of southwestern Atlantic sea surface temperatures during the last century: Cabo Frio continental shelf (Brazil). Palaeogeogr. Palaeoclimatol. Palaeoecol. http://dx.doi.org/10.1016/j.palaeo.2014.01.020.

Duplessy, J., Labeyrie, L., Juillet-Leclerc, A., 1991. Surface salinity reconstruction of the North Atlantic Ocean during the last glacial maximum. Oceanol. Acta 311–324.

Erez, J., Honjo, S., 1981. Comparison of isotopic composition of planktonic foraminifera in plankton tows, sediment traps, and sediments. Palaeogeogr. Palaeoclimatol. Palaeoecol. 33 (1–3), 129–156.

Ezard, T.H.G., Edgar, K.M., Hull, P.M., 2015. Environmental and biological controls on size-specific $\delta^{13}C$ and $\delta^{18}O$ in recent planktonic foraminifera. Paleoceanography 151–173. http://dx.doi.org/10.1002/2014PA002735.

Fairbanks, R.G., Wiebe, P., 1980. Foraminifera and chlorophyll maximum: vertical distribution, seasonal succession, and paleoceanographic significance. Science 209, 1524–1525 (80-.).

Farmer, E.C., Kaplan, A., de Menocal, P.B., Lynch-Stieglitz, J., 2007. Corroborating ecological depth preferences of planktonic foraminifera in the tropical Atlantic with the stable oxygen isotope ratios of core top specimens. Paleoceanography 22http://dx.doi.org/10.1029/2006PA001361. (n/a-n/a).

Franchito, S.H., Rao, V.B., Stech, J.L., Lorenzzetti, J.A., 1998. The effect of coastal upwelling on the sea-breeze circulation at Cabo Frio, Brazil: a numerical experiment. Ann. Geophys. 16, 866–881. http://dx.doi.org/10.1007/s005850050656.

Gibson, K.A., Thunell, R.C., Machain-Castillo, M.L., Fehrenbacher, J., Spero, H.J., Wejnert, K., Nava-Fernandez, X., Tappa, E.J., 2016. Evaluating controls on planktonic foraminiferal geochemistry in the Eastern Tropical North Pacific. Earth Planet. Sci. Lett. 452, 90–103. http://dx.doi.org/10.1016/j.epsl.2016.07.039.

Goswami, S., 2004. Zooplankton methodology, collection & identyification - a field manual. Natl Inst. Oceanogr. 16.

Hut, G., 1987. Consultants' group meeting on stable isotope reference samples for geochemical and hydrological investigations. Rep. Dir. Gen. 16–18 (doi:18075746).

Ikeda, Y., Miranda, L.B., Rock, N.J., 1974. Observations on stages of upwelling in the region of Cabo Frio (Brazil) as conducted by continuous surface temperature and salinity measurements. Bol. do Inst. Ocean. São Paulo 23, 33–46.

Jonkers, L., Kucera, M., 2015. Global analysis of seasonality in the shell flux of extant planktonic foraminifera. Biogeosciences 1327–1372. http://dx.doi.org/10.5194/bgd-12-1327-2015.

Jonkers, L., Brummer, G.J.A., Peeters, F.J.C., Van Aken, H.M., De Jong, M.F., 2010. Seasonal stratification, shell flux, and oxygen isotope dynamics of left coiling *N. pachyderma* and *T. quinqueloba* in the western subpolar North Atlantic. Paleoceanography 25, 1–13. http://dx.doi.org/10.1029/2009PA001849.

King, A.L., Howard, W.R., 2005. $\delta^{18}O$ seasonality of planktonic foraminifera from Southern Ocean sediment traps: latitudinal gradients and implications for paleoclimate reconstructions. Mar. Micropaleontol. 56, 1–24. http://dx.doi.org/10.1016/j.marmicro.2005.02.008.

Kucera, M., 2007. Planktonic foraminifera as tracers of past oceanic environments. In: Hillaire-Marcel, C., de Vernal, A. (Eds.), Proxies in Late Cenozoic Paleoceanography. vol. 1. Elsevier, Amsterdam, pp. 213–262. http://dx.doi.org/10.1016/S1572-5480(07)01011-1. (chap. 6).

Lessa, D.V. de O., Ramos, R.P., Barbosa, C.F., da Silva, A.R., Belem, A., Turcq, B., Albuquerque, A.L., 2014. Planktonic foraminifera in the sediment of a western boundary upwelling system off Cabo Frio, Brazil. Mar. Micropaleontol. 106, 55–68. http://dx.doi.org/10.1016/j.marmicro.2013.12.003.

Lessa, D.V., Venancio, I.M., dos Santos, T.P., Belem, A.L., Turcq, B.J., Sifeddine, A., Albuquerque, a.L.S., 2016. Holocene oscillations of Southwest Atlantic shelf circulation based on planktonic foraminifera from an upwelling system (off Cabo Frio, southeastern Brazil). The Holocene. http://dx.doi.org/10.1177/0959683616638433.

Lopes, R.M., Katsuragawa, M., Dias, J.F., Monica, A., Muelbert, J.H., Gorri, C., Brandini, F.P., 2006. Zooplankton and ichthyoplankton distribution on the southern Brazilian shelf: an overview. Sci. Mar. 70, 189–202.

Mix, A.C., 1987. The oxygen-isotope record of glaciation. In: North America and Adjacent Oceans during the Last Deglaciation, pp. 111–135.

Mulitza, S., Dürkoop, A., Hale, W., Wefer, G., Niebler, H.S., 1997. Planktonic foraminifera as recorders of past surface-water stratification. Geology 25, 335–338. http://dx.doi.org/10.1130/0091-7613(1997)025<0335.

Mulitza, S., Wolff, T., Pgtzold, J., Hale, W., Wefer, G., 1998. Temperature sensitivity of planktic foraminifera and its influence on the oxygen isotope record. Mar. Micropaleontol. 33, 223–240.

Peterson, R.G., Stramma, L., 1991. Upper-level circulation in the South Atlantic Ocean. Prog. Oceanogr. 26, 1–73. http://dx.doi.org/10.1016/0079-6611(91)90006-8.

Pierre, C., Vergnaud-grazzini, C., Faughres, J., 1991. Oxygen and carbon stable isotope tracers of the water masses in the Central Brazil Basin. Deep Sea Res. Part A 38, 597–606.

Portilho-Ramos, R. da C., Ferreira, F., Calado, L., Frontalini, F., de Toledo, M.B., 2015. Variability of the upwelling system in the southeastern Brazilian margin for the last 110,000 years. Glob. Planet. Chang. 135, 179–189. http://dx.doi.org/10.1016/j.gloplacha.2015.11.003.

Ravelo, A.C., Fairbanks, R.G., 1992. Oxygen isotopic composition of multiple species of planktonic foraminifera: recorders of the modern photic zone temperature gradient. Paleoceanography 7, 815–831. http://dx.doi.org/10.1029/92PA02092.

Ravelo, A.C., Fairbanks, R.G., Philander, S.G.H., 1990. Distributions in plankton tows, the species foraminifera abundances in core tops correlate with observations of modern photic zone hydrography defined here as seasonal temperature variation and mixed layer depth. The hydrography is mathematically descri. 5, 409–431.

Rebotim, A., Voelker, A.H.L., Jonkers, L., Waniek, J.J., Meggers, H., Schiebel, R., Fraile, I., Schulz, M., Kucera, M., 2017. Factors controlling the depth habitat of planktonic foraminifera in the subtropical eastern North Atlantic. Biogeosciences 14, 827–859. http://dx.doi.org/10.5194/bg-2016-348.

Rodrigues, R.R., Lorenzzetti, J.a., 2001. A numerical study of the effects of bottom topography and coastline geometry on the Southeast Brazilian coastal upwelling. Cont. Shelf Res. 21, 371–394. http://dx.doi.org/10.1016/S0278-4343(00)00094-7.

Sagawa, T., Kuroyanagi, A., Irino, T., Kuwae, M., Kawahata, H., 2013. Seasonal variations in planktonic foraminiferal flux and oxygen isotopic composition in the western North Pacific: Implications for paleoceanographic reconstruction. Mar. Micropaleontol. 100, 11–20. http://dx.doi.org/10.1016/j.marmicro.2013.03.013.

Schmuker, B., Schiebel, R., 2002. Planktic foraminifers and hydrography of the eastern and northern Caribbean Sea. Mar. Micropaleontol. 46, 387–403. http://dx.doi.org/10.1016/S0377-8398(02)00082-8.

Siccha, M., Trommer, G., Schulz, H., Hemleben, C., Kucera, M., 2009. Factors controlling the distribution of planktonic foraminifera in the Red Sea and implications for the development of transfer functions. Mar. Micropaleontol. 72, 146–156. http://dx.doi.org/10.1016/j.marmicro.2009.04.002.

Silveira, I.C.A., Schmidt, A., Campos, E.J.D., Godoi, S.S. De, Ikeda, Y., 2000. A Corrente do Brasil ao Largo da Costa Leste Brasileira. Rev. Bras. Oceanogr. 48, 171–183.

Silveira, I.C.A., Lima, J.A.M., Schmidt, A.C.K., Ceccopieri, W., Sartori, A., Franscisco, C.P.F., Fontes, R.F.C., 2008. Is the meander growth in the Brazil Current system off Southeast Brazil due to baroclinic instability? Dyn. Atmos. Oceans 45, 187–207. http://dx.doi.org/10.1016/j.dynatmoce.2008.01.002.

Simstich, J., Sarnthein, M., Erlenkeuser, H., 2003. Paired $\delta^{18}O$ signals of neogloboquadrina pachyderma(s) and *Turborotalita quinqueloba* show thermal stratification structure in Nordic seas. Mar. Micropaleontol. 48, 107–125. http://dx.doi.org/10.1016/S0377-8398(02)00165-2.

Sousa, S.H.M., de Godoi, S.S., Amaral, P.G.C., Vicente, T.M., Martins, M.V.A., Sorano, M.R.G.S., Gaeta, S.A., Passos, R.F., Mahiques, M.M., 2014. Distribution of living planktonic foraminifera in relation to oceanic processes on the southeastern continental Brazilian margin (23°S–25°S and 40°W–44°W). Cont. Shelf Res. 89, 76–87. http://dx.doi.org/10.1016/j.csr.2013.11.027.

Souto, D.D., de Oliveira Lessa, D.V., Albuquerque, A.L.S., Sifeddine, A., Turcq, B.J., Barbosa, C.F., 2011. Marine sediments from southeastern Brazilian continental shelf: a 1200 year record of upwelling productivity. Palaeogeogr. Palaeoclimatol. Palaeoecol. 299, 49–55. http://dx.doi.org/10.1016/j.palaeo.2010.10.032.

Spezzaferri, S., Kucera, M., Pearson, P.N., Wade, B.S., Rappo, S., Poole, C.R., Morard, R., Stalder, C., 2015. Fossil and genetic evidence for the polyphyletic nature of the planktonic foraminifera “Globigerinoides”, and description of the new genus *Trilobatus*. PLoS One 10, 1–20. http://dx.doi.org/10.1371/journal.pone.0128108.

Steph, S., Regenberg, M., Tiedemann, R., Mulitza, S., Nürnberg, D., 2009. Stable isotopes of planktonic foraminifera from tropical Atlantic/Caribbean core-tops: implications for reconstructing upper ocean stratification. Mar. Micropaleontol. 71, 1–19. http://dx.doi.org/10.1016/j.marmicro.2008.12.004.

Stramma, L., England, M., 1999. On the water massed and mean circulation of the South Atlantic Ocean. J. Geophys. Res. 104, 20863–20883.

Tedesco, K., Thunell, R., Astor, Y., Muller-karger, F., 2007. The oxygen isotope composition of planktonic foraminifera from the Cariaco Basin, Venezuela: seasonal and interannual variations. Mar. Micropaleontol. 62, 180–193. http://dx.doi.org/10.1016/j.marmicro.2006.08.002.

Thunell, R., Sautter, L.R., 1992. Planktonic foraminiferal faunal and stable isotopic indices of upwelling: a sediment trap study in the San Pedro Basin, Southern California Bight. Geol. Soc. Lond. Spec. Publ. 64, 77–91. http://dx.doi.org/10.1144/GSL.SP.1992.064.01.05.

Toledo, F.A.L., Costa, K.B., Pivel, M.A.G., 2007. Salinity changes in the western tropical South Atlantic during the last 30 kyr. Glob. Planet. Chang. 57, 383–395. http://dx.doi.org/10.1016/j.gloplacha.2007.01.001.

Ufkes, E., Jansen, J.H.F., Brummer, G.J.A., 1998. Living planktonic foraminifera in the eastern South Atlantic during spring: indicators of water masses, upwelling and the Congo (Zaire) river plume. Mar. Micropaleontol. 33, 27–53. http://dx.doi.org/10.1016/S0377-8398(97)00032-7.

Valentin, J.L., 2001. The Cabo Frio upwelling system, Brazil. In: Seeliger, U., Kjerfve, B. (Eds.), Coastal Marine Ecosystems of Latin America. Springer, Berlin, Heidelberg, pp. 97–105.

Venancio, I.M., Belem, A.L., dos Santos, T.H.R., Zucchi, M.D.R., Azevedo, A.E.G., Capilla, R., Albuquerque, A.L.S., 2014. Influence of continental shelf processes in the water mass balance and productivity from stable isotope data on the southeastern Brazilian coast. J. Mar. Syst. 139, 241–247. http://dx.doi.org/10.1016/j.jmarsys.2014.06.009.

Venancio, I.M., Franco, D., Belem, A.L., Mulitza, S., Siccha, M., Albuquerque, A.L.S., Schulz, M., Kucera, M., 2016a. Planktonic foraminifera shell fluxes from a weekly resolved sediment trap record in the southwestern Atlantic: evidence for synchronized reproduction. Mar. Micropaleontol. 125, 25–35. http://dx.doi.org/10.1016/j.marmicro.2016.03.003.

Venancio, I.M., Gomes, V.P., Belem, A.L., Albuquerque, A.L.S., 2016b. Surface-to-subsurface temperature variations during the last century in a western boundary upwelling system (southeastern, Brazil). Cont. Shelf Res. 125, 97–106. http://dx.doi.org/10.1016/j.csr.2016.07.003.

Vicalvi, M.A., 1997. Zoneamento bioestratigráfico e paleoclimático dos sedimentos do quaternário superior do talude da bacia de Campos, RJ, Brazil. Bol. Geociênc. Petrobras 11, 132–165 (K).

Walsh, J.J., 1988. On the Nature of Continental Shelves. Academic Press, New York.

Wejnert, K.E., Thunell, R.C., Astor, Y., 2013. Comparison of species-specific oxygen isotope paleotemperature equations: sensitivity analysis using planktonic foraminifera from the Cariaco Basin, Venezuela. Mar. Micropaleontol. 101, 76–88. http://dx.doi.org/10.1016/j.marmicro.2013.03.001.

Williams, D.F., Healy-Williams, N., 1980. Oxygen isotopic-hydrographic relationships among recent planktonic foraminifera from Indian Ocena. Nature 283, 848–852. http://dx.doi.org/10.1038/283848a0.

Žarić, S., Donner, B., Fischer, G., Mulitza, S., Wefer, G., 2005. Sensitivity of planktic foraminifera to sea surface temperature and export production as derived from sediment trap data. Mar. Micropaleontol. 55, 75–105. http://dx.doi.org/10.1016/j.marmicro.2005.01.002.